

# **Largen: A Molecular Regulator of Mammalian Cell Size Control**

**Kazuo Yamamoto,<sup>1,2,8</sup> Valentina Gandin,<sup>3</sup> Masato Sasaki,<sup>1,2</sup> Susan McCracken,<sup>1,2</sup> Wanda Li,<sup>1,2</sup> Jennifer Liepa Silvester,<sup>1,2</sup> Andrew J. Elia,<sup>1,2</sup> Feng Wang,<sup>2,4</sup> Yosuke Wakutani,<sup>5</sup> Roumiana Alexandrova,<sup>1</sup> Yathor D Oo,<sup>2</sup> Peter Mullen,<sup>6</sup> Satoshi Inoue,<sup>1,2</sup> Momoe Itsumi,<sup>1,2</sup> Valentina Lapin,<sup>1,2</sup> Jillian Haight,<sup>1,2</sup> Andrew Wakeham,<sup>1,2</sup> Arda Shahinian,<sup>1,2</sup> Mitsuhiro Ikura,<sup>2,4</sup> Ivan Topisirovic,<sup>3</sup> Nahum Sonenberg<sup>7</sup> and Tak W. Mak<sup>1,2,\*</sup>**

<sup>1</sup>The Campbell Family Cancer Research Institute, Ontario Cancer Institute, University Health Network, Toronto, Ontario M5G 2C1, Canada

<sup>2</sup>Departments of Medical Biophysics and Immunology, University of Toronto, Toronto, Ontario M5S 1A8, Canada

<sup>3</sup>Lady Davis Institute for Medical Research, Sir Mortimer B. Davis Jewish General Hospital, and Department of Oncology, McGill University, Montreal, Quebec H3T 1E2, Canada

<sup>4</sup>Division of Signaling Biology, Ontario Cancer Institute, Toronto, Ontario M5G 1L7, Canada

<sup>5</sup>Department of Neurology, Kurashiki Heisei Hospital, Kurashiki, Okayama 710-0826, Japan

<sup>6</sup>Division of Cancer Genomics and Proteomics, Ontario Cancer Institute, Toronto, Ontario M5G 2M9, Canada

<sup>7</sup>Department of Biochemistry, McGill University, Montreal, Quebec H3A 1A3, Canada

<sup>8</sup>Present address: Biomedical Research Support Center, Nagasaki University School of Medical Sciences, 1-12-4 Sakamoto, Nagasaki, Nagasaki 852-8523, Japan

\*Correspondence:

Tak W. Mak, Director

The Campbell Family Cancer Research Institute

620 University Avenue, Suite 706, Toronto, ON, Canada M5G 2C1

Telephone: 416-946-2234 Fax: 416-204-5300 Email: [tmak@uhnresearch.ca](mailto:tmak@uhnresearch.ca)

**Running Title:** Largen controls mammalian cell size

## **SUMMARY**

Little is known about how mammalian cells maintain cell size homeostasis. We conducted a novel genetic screen to identify cell size-controlling genes and isolated Largen, the product of a gene (*PRR16*) that increased cell size upon overexpression in human cells. *In vitro* evidence indicated that Largen preferentially stimulates the translation of specific subsets of mRNAs, including those encoding proteins affecting mitochondrial functions. The involvement of Largen in mitochondrial respiration was consistent with the increased mitochondrial mass and greater ATP production in Largen-overexpressing cells. Furthermore, Largen overexpression led to increased cell size *in vivo*, as revealed by analyses of conditional Largen transgenic mice. Our results establish Largen as an important link between mRNA translation, mitochondrial functions, and the control of mammalian cell size.

## **Highlights**

PRR16/Largen is identified in a screen for genes controlling mammalian cell size.

Largen enhances mRNA translation.

Largen increases mitochondrial mass and activity.

Largen controls cell size *in vivo*.

## INTRODUCTION

The human body consists of 60 billion cells of various shapes and sizes. While differentiated cells tend to have a confined range of size distribution (Altman and Katz, 1976), they can be larger in metabolically active organs (Schmidt and Schibler, 1995), at certain stages of cell maturation or differentiation (Cancro, 2004), during wound healing (Kim et al., 2006), or as a result of asymmetric cell division (Yamashita et al., 2007). These observations suggest that cells have mechanisms to sense and control their size according to their circumstances.

Cell size mutants were first isolated in yeast (Fantès and Nurse, 1977; Jonston et al., 1977; Nurse, 2000). Systematic generation of deletion mutants has since identified hundreds of genes that influence cell size in this organism (Jorgensen et al., 2002; Zhang et al., 2002). Analogous systematic screens performed in *Drosophila* using dsRNA targeting (Bjorklund et al., 2006; Guertin et al., 2006) revealed the unexpected importance in cell size control of the mTOR (mechanistic target of rapamycin) signaling pathway (Cook and Tyers, 2007). mTOR is a serine/threonine kinase known to play a critical role in cell proliferation (Laplanche and Sabatini, 2012; Loewith and Hall, 2011). Growth-regulating signals converge on this kinase, which then directs downstream signaling through either mTOR complex 1 (mTORC1) or mTORC2.

Two mTORC1 substrates, namely S6 kinase 1 and 2 (S6K1, 2), as well as three eIF4E-binding proteins (4E-BP1, 2, and 3), regulate translation initiation (Ma and Blenis, 2009; Magnuson et al., 2012). In contrast, mTORC2 phosphorylates various AGC kinases, including Akt, SGK1 and PKC $\alpha$ , that regulate cell survival and anabolism (Oh and Jacinto., 2011). Interestingly, cells in which mTOR activity is inhibited by rapamycin (RAP) show a

substantial reduction in cell size (Fingar et al., 2002). We took advantage of this phenomenon to design a genetic system to pinpoint genes that could counteract the effects of RAP on cell size. We have identified PRR16/Largen as a novel regulator of cell size that stimulates translation programs and mitochondrial activity. Importantly, Largen acts independently of the two known cell growth regulatory pathways mediated by mTOR and Hippo.

## RESULTS

### Genetic Screen to Identify Genes Controlling Cell Size

We tested various cell lines in pilot studies to confirm that RAP could reduce their size. We chose Jurkat cells for our screen because this cell line showed little variation in cell size distribution under normal conditions and demonstrated a consistent 8-12% size reduction when treated with RAP (Figure S1A, available on-line). We then combined RAP treatment with a novel genetic switch capable of randomly activating any gene in a mammalian genome and looked for genes altering cell size. Our protocol consisted of 4 stages (Figure 1A): (1) mutagenesis of Jurkat cells using the enhanced retroviral mutagen (ERM) system (Liu and Songyang, 2008); (2) treatment of the mutagenized cells with RAP to shrink their size; (3) passage of the RAP-treated mutagenized cells through a fluorescence-activated cell sorter (FACS) to recover a “large cell” population as defined by forward scattering (FSC); and (4) identification of size-controlling genes in single cell clones by reverse transcription-PCR (RT-PCR) and BLAST searching. We hypothesized that if the overexpression of a particular gene was sufficient to overcome the effects of RAP, these mutant cells should stay large even in the presence of RAP, and thus might be isolated simply by sorting for the largest cells.

When the ERM provirus is integrated in the host cell genome, the hemagglutinin (HA)-tag is transcribed by the tetracycline (Tet)-responsive promoter within the provirus under the control of the Tet-sensitive transactivator tTA. Due to a consensus splicing donor sequence positioned after the HA-tag, this short segment forms chimeric transcripts with

downstream exons of the endogenous gene where the provirus is inserted. As a result, the chimeric transcripts are constitutively overexpressed in the host cell but can be shut off by the tetracycline derivative doxycycline (DOX). In some cases, recruitment of tTA to the provirus integration site fortuitously activates transcription from the intrinsic promoter, which is also controllable by DOX. We infected stable tTA-expressing Jurkat cells with ERM virus, applied puromycin to select virus-infected cells, and added 20 nM RAP for 2 days. The top 1-2% largest cells were collected by FACS and cultured as a pool. This cycle was repeated 3 times to concentrate “stay-large” mutants (Figure S1B). Importantly, this phenotype was reversed by DOX treatment (Figure S1C). Thus, our genetic screen successfully enriched for “large cell” mutants whose phenotype depended on the overexpression of a gene induced by ERM integration.

When we isolated single cell clones from the mutant pools by limiting dilution, we found that some showed less reduction in cell size upon RAP treatment than controls, and that all revealed more RAP sensitivity upon DOX treatment (Figure S1D). We selected several clones that “stayed large” in the presence of RAP and mapped their ERM integration sites using RT-PCR (Table S1). The most frequently identified locus of integration was 8q24.21, the region between *c-myc* and *gasdermin-C*, but no significant transcriptional activation of either of these genes was observed (data not shown). Other clones, such as clone 1C2, showed an increase in cell size that did not change with RAP and did not depend on DOX (Figure 1B). Although *C1orf186* was strongly expressed in untreated clone 1C2, the induction of this gene was poorly suppressed by DOX (Figure 1C). In contrast, clones 2D10

and 3B3 showed a marginal reduction in cell size with RAP but became more sensitive to RAP after DOX treatment (Figure 1B). In these two clones, the ERM was integrated at 5q23.1 between the mitochondrial ferritin gene and a gene called “proline-rich protein 16” (*PRR16*). The only transcript overexpressed in both 2D10 and 3B3 cells contained sequences derived from *PRR16*, and the expression of this transcript was readily reverted by DOX (Figures 1C and 1D). Determination of the mean volumes of 3B3 and 2D10 cells confirmed that they were already larger than parental Jurkat cells in the absence of RAP (Figures 1E and S1E). RAP induced a small reduction in cell volume in these two clones that was enhanced by DOX treatment (Figure 1E). These results suggested that the protein product of the *PRR16* gene overexpressed in these clones was a potential regulator of mammalian cell size.

### **PRR16/Largen Controls Mammalian Cell Size**

To confirm our screening results, we stably overexpressed the human *PRR16* gene as a GFP fusion protein in Jurkat cells and treated them (or not) with RAP. Overexpression of the GFP fusion protein (Figure S2A) increased Jurkat cell size compared to control cells overexpressing GFP only (Figure 2A). While RAP reduced the size of both GFP- and GFP-*PRR16*-overexpressing cells, the latter were still larger than the former (Figure 2A). However, the size reductions induced by RAP in both types of cells were similar in range (11-12%), suggesting that the cell size increase induced by *PRR16* overexpression operates in parallel to mTOR signaling. The ability of the *PRR16* gene product to increase cell size was

also demonstrated in HeLa and 293T cells transiently expressing a Myc-tagged version of the protein (Figure S2B), and in 293T cells stably transformed with Myc-tagged PRR16 (Figure S2C). Conversely, when *PRR16* expression was knocked down by siRNA (Figure S2D) in Jurkat, HeLa and 293T cells, cell size was decreased as compared to control siRNA-treated cells (Figures 2B, S2E and S2F). *PRR16* knockdown also resulted in a modest increase in cells positive for Annexin V-propidium iodide staining (Figure S2G), indicating that this gene contributes to cell viability. Sequence analysis showed that *PRR16* encodes an evolutionarily conserved 304 amino acid protein with high (15.8%) proline content (Figure S3). No other structural features or physiological functions of this protein have been reported to date. Because overexpression of the *PRR16* gene rendered cells large, we called its protein product “Largen”.

### **Largen Acts Independently of mTOR and Hippo**

Because we used RAP for our screen, and Largen-overexpressing (O/E) cells were still larger than controls in the presence of RAP, we initially speculated that Largen might modulate mTOR signaling. However, neither the quantity nor phosphorylation status of any mTOR signaling component was affected in 2D10 cells (Figure S4A). We next investigated the potential interaction of Largen with mTOR complexes using co-immunoprecipitation. Myc-tagged PRAS40 was used as a control because PRAS40 is known to bind to mTORC1 (Fonseca et al., 2007; Sancak et al., 2007; Vander Haar et al., 2007). We found that Myc-PRAS40 co-immunoprecipitated with mTOR and Raptor but not with Rictor (Figure 3A),



consistent with previous reports (Fonseca et al., 2007; Sancak et al., 2007; Vander Haar et al., 2007). Neither Raptor nor Rictor bound to Largen, confirming that Largen is not a component of mTOR complexes.

The Hippo pathway is also a key regulator of cell growth (Hervey et al., 2013), which prompted us to investigate whether the effects of Largen on cell size were mediated by Hippo. However, no significant interaction of Largen with any Hippo signaling pathway component examined was observed (Figure S4B). Collectively, these results indicate that the effects of Largen on cell size are largely independent of both the mTOR and Hippo pathways.

### **Largen Affects mRNA Translation**

We noticed that the protein concentrations of 2D10 cell lysates were always much higher than controls (Figure 3B), implying that Largen might regulate mRNA translation. We therefore compared the rate of incorporation of [<sup>35</sup>S]-methionine (<sup>35</sup>S-Met) into total protein in 2D10 and Jurkat cells. RAP treatment reduced <sup>35</sup>S-Met incorporation in Jurkat cells by ~40%, and DOX treatment did not significantly alter this tendency (Figure 3C). Untreated 2D10 cells showed a ~1.8-fold higher translation rate than Jurkat cells, and this rate was reduced to the same extent by RAP. DOX treatment alone reduced the translation rate in 2D10 cells by ~20%, whereas a combination of DOX and RAP drastically decreased this rate. We also examined translation rates in Largen-O/E or Largen knockdown 293T and HeLa cells. In both cell lines, Largen overexpression enhanced <sup>35</sup>S-Met incorporation,

whereas Largen knockdown modestly but reproducibly reduced it (Figure 3D). Taken together, these results suggest that Largen regulates translation in a mTOR-independent manner.

We confirmed the above observations by an alternative assay that used a reporter plasmid to measure the efficiency of mRNA translation (Ueda et al., 2004). The firefly (FF) luciferase activity directed by this plasmid reflects the translation rate after normalization to the mRNA level of the FF reporter gene. We found that Largen-O/E 293T cells exhibited greater FF luciferase activity than controls (Figure 3E), whereas Largen-knockdown 293T cells showed reduced FF luciferase activity (Figure 3F). RAP decreased FF luciferase activity in control 293T cells (Figure 3G), consistent with the previous observation that RAP inhibits cap-dependent translation (Beretta et al., 1996). In our Largen-O/E 293T cells, RAP again reduced FF luciferase activity, but it was still higher than that in the control cells (Figure 3G). Thus, Largen appears to exert a positive effect on mRNA translation that occurs in an mTOR-independent manner and allows cells to compensate for a RAP-induced reduction in cell size.

To assess how Largen affects mRNA translation, we asked if Largen interacts with translation initiation factors. Lysates of 293T cells stably transformed by a Myc-tagged Largen-O/E plasmid or control empty vector were incubated with anti-Myc antibody beads (Figure 3A). Among several translation initiation proteins tested, only minute amounts of eIF4A, eIF4B and eIF4E were detected in Largen immunoprecipitates. This result suggests that Largen affects mRNA translation via a mechanism that does not require direct

interaction with translation initiation factors (see Discussion).

### **Largen Enhances the Translation of Specific Subsets of mRNAs**

We next investigated the effects of Largen overexpression on the translome, the genome-wide pool of actively translated mRNAs (Greenbaum et al., 2001). We isolated light (L; 1-3 ribosomes) and heavy (H; 4 and more ribosomes) polysomes from control and Largen-O/E cells by centrifugation in sucrose density gradients (Figure S5A). We first determined the relative abundance of individual mRNAs in H versus L polysome fractions by microarray and calculated the H:L ratio in control and Largen-O/E cells. Typically, an mRNA with a higher H:L ratio is loaded onto more ribosomes and is thus translated more efficiently than an mRNA exhibiting a lower H:L ratio (Warner et al., 1963). When we analyzed mRNAs with a high H:L ratio in control and Largen-O/E cells, we found that 251 genes were selectively upregulated in Largen-O/E cells at a threshold H:L ratio of >3.5-fold (Table S2). Of these 251 transcripts, 34 corresponded to histone clusters and 25 encoded mitochondrial proteins (Figures 4A, S5B, and Table S2). Enrichment of the mRNAs for histone H3A (HIST2H3A), mitochondrial ribosome protein L49 (MRPL49), and NADH dehydrogenase (ubiquinone) Fe-S protein 5 (NDUFS5) in the heavy polysome fractions of Largen-O/E cells was confirmed by quantitative real time-PCR (qRT-PCR) (Figure 4B). In contrast, the distribution of mRNAs with a low H:L ratio (<2.0), such as that for the housekeeping gene  $\alpha$ -tubulin, was comparable in control and Largen-O/E cells. Interestingly, although the polysomal profiles of control and Largen-O/E cells were almost identical under standard

culture conditions, RAP induced Largen-O/E cells to accumulate more heavy polysomes than control cells (Figure S5C). Consistent with this observation, the HIST2H3A, MRPL49 and NDUF55 mRNAs shifted to lighter polysome fractions or were released from ribosomes in RAP-treated control cells, but remained in heavy polysome fractions in RAP-treated Largen-O/E cells (Figure 4B). Immunoblotting confirmed that concentrations of the MRPL49 and NDUF55 polypeptides, as well as the related proteins MRPL3 and NDUFA8, were increased by Largen overexpression (Figures 4C and S5D). The enhanced translation of these mRNAs encoding mitochondrial proteins was even more obvious when mitochondrial extracts were examined (Figure S5E).

### **Largen Increases Mitochondrial Mass and Respiration**

The observation that a set of mitochondrial proteins was specifically increased in 2D10 cells prompted us to investigate the quality and quantity of mitochondria in Largen-O/E cells. We transformed 293T cells with either a Myc-tagged Largen-IRES-EGFP plasmid or a control IRES-EGFP vector. We found that two independent lines of GFP<sup>+</sup> Largen-O/E 293T cells stained more brightly with Mitotracker, a mitochondrion-specific dye, than did the GFP<sup>+</sup> control cell line (Figure 5A), a finding confirmed semi-quantitatively by flow cytometry (Figure 5B). In addition, when we used Mitotracker-Green to measure mitochondrial mass in 2D10 cells, these mutants stained more intensely than parental Jurkat cells (Figure 5C). The ratio of mitochondrial DNA (mtDNA) to nuclear DNA (ncDNA) was also increased in 2D10 cells (Figure 5D), as was mitochondrial respiration as determined by the oxygen consumption

rate (Figure 5E). Consistent with these findings, 2D10 cells produced more ATP than controls (Figure 5F), as did untreated Largen-O/E 293T cells (Figure 5G). Interestingly, the RAP-induced reduction of ATP production in control 293T cells was attenuated by Largen overexpression (Figure 5G). Collectively, these observations indicate that Largen overexpression increases both mitochondrial mass and activity.

### **Mitochondrial Respiration Is Linked to Cell Size Control**

The data presented above suggested that mitochondrial respiration, ATP production and cell size regulation are connected. To investigate this hypothesis, we measured cell size changes in the presence of the respiratory inhibitor carbonyl cyanide 4-(trifluoromethoxy) phenylhydrazone (FCCP), which chemically uncouples electron transport and oxidative phosphorylation. Cells in which mitochondrial activity is upregulated are partially resistant to FCCP (Strohecker et al., 2013; Szabo et al., 2013). We found that FCCP treatment of Jurkat cells reduced their cell size (Figure 6A) in a manner that was not affected by DOX (Figure 6B). In contrast, DOX-treated 2D10 cells, in which Largen overexpression was shut off, showed a greater degree of cell size reduction in response to FCCP than 2D10 cells that were not treated with DOX (Figure 6B). These data indicate that the enhanced mitochondrial activity induced by Largen overexpression can attenuate FCCP-dependent cell size reduction, and support our tenet that mitochondrial activity plays an important role in mammalian cell size regulation.

## **Largen Overexpression Increases Cell Size *In Vivo***

To investigate the effects of Largen overexpression *in vivo*, we created Largen transgenic (Tg) mice. However, systemic overexpression of this protein was early embryonic lethal in the C57Bl/6 background (data not shown). We therefore used the Cre recombinase-*loxP* system to generate conditional Largen-Tg mice. We crossed these mutants to Tg strains expressing Cre under the control of the albumin promoter (Postic and Magnuson, 2000), or the muscle creatine kinase promoter (Wang et al., 1999), to generate progeny with liver-specific Largen expression (Largen-AlbCre mice) or heart- and muscle-specific Largen expression (Largen-CkmmCre mice), respectively. Largen-AlbCre and Largen-CkmmCre mice were born at the expected Mendelian ratio and grew normally (data not shown). Liver-specific Largen overexpression increased the average size of hepatocytes in Largen-AlbCre mice compared to littermate controls (Figures 7A and 7B), and Largen-O/E hepatocytes showed a higher mtDNA copy number (Figure 7C). Interestingly, despite the increase in hepatocyte size, the ratio of liver weight to body weight was normal in Largen-AlbCre mice (Figure 7D), as was the ratio of heart weight to body weight in Largen-CkmmCre mice (data not shown). However, when the mean cross-sectional area of cardiomyocytes in control and Largen-CkmmCre mice was compared, the average size of cardiomyocytes was significantly increased in Largen-CkmmCre mice (Figures 7E and 7F). Taken together, these results establish that Largen influences mammalian cell size not only in cell cultures but also in whole animals.

## DISCUSSION

We report here the identification of a novel protein Largen, encoded by the *PRR16* gene, as a regulator of mammalian cell size. Previous systematic genetic screens to elucidate mechanisms underlying cell size homeostasis have relied on loss-of-function phenotypes, a strategy that runs the risk of missing genes that are essential not only for cell size regulation but also for cell viability (Bjorklund et al., 2006; Guertin et al., 2006; Jorgensen et al., 2002; Sims et al., 2009; Zhang et al., 2002) We have conducted a gain-of-function screen using the ERM system (Liu and Songyang, 2008), which is a more sophisticated approach and better suited for assessing an intricate genetic circuit like cell size regulation. Importantly, because our methodology was designed for mammalian cell cultures, we succeeded in identifying Largen despite the fact that Largen orthologues do not appear to exist in yeast, fly or worm. Significantly, Largen is highly conserved in vertebrates, including in zebrafish (Figure S3). The Largen C-terminus shows less diversity than the N-terminus, and several splice variants encoding divergent N-terminal regions can be found in human and mouse databases (data not shown).

The *PRR16* gene was initially described as encoding DSC54, a mesenchymal stem cell marker protein (Barberi et al., 2005) that is also expressed in human placental endothelial cells (Lang et al., 2008). This gene was subsequently renamed in genomic databases as “proline-rich protein 16” because of its relatively high proline content (Figure S3). Protein-protein interaction studies have identified the protein encoded by *PRR16* as a binding partner for ubiquitin ligase Nedd4 *in vitro* (Persaud et al., 2009) and for protein phosphatase-1 $\alpha$  *in vivo* (Esteves et al., 2012). However, because the physiological

relevance of these interactions is unclear, and our work has clearly demonstrated that the *PRR16* protein product increases cell size *in vivo*, we believe we are justified in naming this protein “Largen”.

It has long been known that cell size correlates with intracellular protein level (Bales et al., 1988; Crissman and Steinkamp, 1973). Accordingly, we found that Largen overexpression stimulated mRNA translation and resulted in protein accumulation (Figures 3C-G). Our polysomal profiling experiments demonstrated the unique effects of Largen on the translome. Largen-O/E cells contained 251 unique transcripts enriched by >3.5-fold in heavy polysome fractions. About one-third of these transcripts encoded histones, mitochondrial proteins, or vesicular transport proteins (Figure S5B; Table S2). While most histone mRNAs were from the H1 and H2 clusters, histone H3 transcripts showed one of the highest fold-change values, consistent with the accumulation of histone H3 proteins in Largen-O/E cells (Figure 4B and data not shown). A recent genome-wide characterization of mRNA translation has revealed that the translation of histone mRNAs proceeds even when mTOR is inhibited by the ATP-competitive inhibitor Torin-1 (Thoreen et al. 2012). Histone mRNAs have unusually short 5'-untranslated regions (UTRs) and no poly-(A) tails, and use a distinct mode of translation initiation that is not stimulated by mTOR (Martin et al., 2011). Our identification of histone mRNA enrichment in heavy polysomes of Largen-O/E cells may reflect these observations, and suggest that Largen may enhance mRNA translation independently of mTOR.

The precise mechanism by which Largen regulates mRNA translation remains



elusive. We have demonstrated that the effects of Largen on mRNA translation are not likely to be mediated via its direct interaction with translation initiation factors, or by effects on the assembly of the eIF4F complex (Figure 3A and data not shown). Considering that mTOR is a major regulator of eIF4F complex assembly (Roux and Topisirovic, 2012), our findings further strengthen our model in which Largen regulates translation independently of mTOR. It remains to be determined whether Largen affects translational programs by indirectly modulating rate-limiting translation initiation factors whose function is largely independent of mTOR (e.g. eIF2), or by stimulating elongation or other translation-related processes such as ribosome biogenesis.

Transcripts encoding 25 mitochondrial proteins were also enriched in heavy polysome fractions of Largen-O/E cells. These proteins are involved in mitochondrial respiration, transcription or translation, or protein transport or folding (Figure 4A). However, only some of the protein components necessary for these processes were elevated in Largen-O/E cells, and these to a variable extent. In addition, some protein components whose mRNAs were not enriched in heavy polysomes of Largen-O/E cells also showed upregulated translation (c.f. ATP5G2, Figure S5E). These results suggest that the elevation of only a few proteins involved in a mitochondrial process or pathway is sufficient to enhance the stability and/or reduce the degradation of other components, leading to an overall increase in both the quality and quantity of mitochondria (Figures 5A-5E). Consistent with this observation, ATP production was increased in Largen-O/E cells (Figures 5F and 5G). Although RAP inhibited ATP production both in control and Largen-O/E cells, the latter

still produced more ATP than untreated controls. This enhanced ATP production may partially explain why RAP-treated Lagen-O/E cells are able to maintain their large size.

How does Lagen upregulate the translation of a specific set of genes? In *Drosophila* subjected to dietary restriction, certain nuclear-encoded mitochondrial genes that showed increased translation had a shorter and less structured 5'-UTR (Zid et al., 2009). So far, we have not found a common genetic signature among our Lagen-controlled mammalian transcripts (data not shown). Coupled with the fact that no obvious Lagen orthologues have been identified in yeast or fly, this finding indicates that a more complicated regulatory mechanism may be responsible for Lagen-dependent enhancement of mammalian mRNA translation. Like Lagen, the mTOR pathway regulates the translation of a subset of nuclear-encoded mitochondrial proteins (Morita *et al.*, 2013). However, there is no significant overlap among mitochondrial proteins that are synthesized in an mTOR- vs Lagen-dependent manner. These findings further corroborate the notion that Lagen regulates translation of mitochondria-related mRNAs independently of mTORC1, and that translational control of mitochondrial energy production plays a major role in the regulation of cell growth in mammals.

Our *in vitro* findings demonstrating that Lagen controls cell size were recapitulated *in vivo* in our tissue-specific Lagen-Tg mice. Hepatocytes were larger in size in Lagen-O/E liver (Figures 7A and 7B). However, the liver:body weight ratio in these mutants was normal (Figure 7D), suggesting that cell size is not a critical determinant of organ size. Several genes in the PI3K-mTOR signaling pathway enhance organ size upon tissue-specific

overexpression (Malstrom et al., 2001; Sengupta et al., 2010; Shioi et al., 2000 and 2002; Tuttle et al., 2001). Constitutively active PI3K in mouse heart increased both the number and size of cardiomyocytes, expanding overall heart size (Shioi et al., 2000). In contrast, constitutively active Akt in mouse heart increased heart weight due to an effect on cell size but not on cell number (Shioi et al., 2002). Overexpression of an alternative constitutively active form of Akt in mouse pancreas increased both the size and number of pancreatic  $\beta$  cells (Tuttle et al., 2001). However, overexpression of this same mutant Akt in thymus increased thymus size but decreased thymocyte numbers such that the thymus weight was normal (Malstrom et al., 2001). Thus, the determination of organ size depends on the tissue context and requires additional factors beyond those exerting cell-autonomous effects (Conlon and Raff, 1999; Yang and Xu, 2011). A candidate may be the Hippo signaling pathway, which coordinates apoptosis and proliferation and so may be mechanistically important for overall organ size determination (Tumaneng et al., 2012).

Our study has identified PRR16/Largen as a gene controlling mammalian cell size independently of mTOR and Hippo, which are the two major regulators of cell size known to date. It is noteworthy to mention that we have observed that Largen-O/E cells grow more slowly than control cells but show no significant differences in cell cycle progression or rate of intracellular protein degradation (Figure S6). These findings are in line with previous reports establishing that cell size and proliferation can be uncoupled (Dowling et al., 2010; Urbani et al., 1995). Although the molecular details of how Largen controls these phenomena remain to be determined, these observations and our findings presented above

suggest a model for the control of mammalian cell size (Figure 7G). Mitochondria produce ATP for use during mRNA translation, the most energy-consuming process within a cell (Rolfe and Brown, 1997). Translation generates the proteins needed for a cell's architectural and metabolic activities, including mitochondrial respiration. Largin may normally ensure the smooth operation of translation such that Largin overexpression accelerates a positive feedback loop, leading to an increase in total cell mass. Additional tissue-specific gene targeting in mice is under way to elucidate the position of Largin in the molecular pathway underlying this feedback loop.

## **EXPERIMENTAL PROCEDURES**

### **ERM and Genetic Screening**

Production and infection of ERM retrovirus was as described (Swift et al., 1999). Jurkat T cells ( $2.4 \times 10^7$ ) were infected with ERM virus, selected in 2  $\mu\text{g}/\text{ml}$  puromycin (Sigma-Aldrich), and treated with 20 nM rapamycin (Cell Signaling Technology) for 2 days prior to FACS and collection of the top 1-2% largest cells. Large cells were expanded in number and passed through the RAP treatment and sorting cycle three more times. Single cell clones were isolated by limiting dilution. Sizes of individual cells were measured by flow cytometry after culture under normal conditions, or after RAP treatment with or without 1  $\mu\text{g}/\text{ml}$  doxycycline (BD Biosciences).

Total RNA prepared from each single cell clone was converted to first strand cDNA using the ProSTAR Ultra HF RT-PCR System (Stratagene) and the RT-1 primer. Using the first strand cDNA as a template, HA-tagged transcript-specific PCR was performed using an HA-specific primer and the RT-0 primer. Amplified PCR products were subcloned into the pCR2.1TOPO vector (Invitrogen). Recombinant plasmids were isolated from 5-10 independent *E. coli* transformants and the inserts were verified by sequencing. The most frequent sequence was taken as representing the gene for each clone, and was subjected to a genomic BLAST search to identify the locus. The primers used for RT-PCR are listed in Table S3.

### **Cell Size Determinations**

For cell size determination by standard flow cytometry, exponentially-growing cells were applied to a FACSCalibur (BD Biosciences) and data were analyzed with CellQuest Pro version 5.2 software (BD Biosciences). The mean forward scatter (FSC) value was used as an estimate of overall cell size. Cell volumes were also measured using a Moxi Z automated cell counter (ORFLO Technologies). For each test, >1000 individual cells were passed through an electric current and the results recorded and presented in histogram format. Cell volume values were calculated as the mean of cell volumes measured in 3 independent experiments.

### **[<sup>35</sup>S]-Methionine Incorporation**

Cells were seeded at  $1 \times 10^5$ /well in 12-well plates and cultured overnight prior to transfection with plasmids or siRNA as described in Supplemental Experimental Procedures. At 2 days post-transfection, cells were washed twice with methionine-free  $\alpha$ -MEM supplemented with 10% dialysed FBS (labeling medium) and incubated in 900  $\mu$ l labeling medium for 45 min at 37°C in 5% CO<sub>2</sub>. Fresh labeling medium (100  $\mu$ l) containing 0.2  $\mu$ l [<sup>35</sup>S]-methionine [ $>1000$ Ci (37.0TBq)/mmol; Perkin Elmer] was added to each well and incubation continued for 30 min. Labeled cells were washed twice with PBS(-) and protein lysates were prepared from  $1 \times 10^5$  cells. Radioactivity in whole lysates was determined using a scintillator counter and values were normalized to total protein and cell number. These values were expressed relative to the value for untreated control cells. Relative normalized values from 3 independent experiments were then combined.

### **Translation Reporter Assay**

Cells were transfected as above with the reporter plasmid pEF-FFL-IRES-fSPL (Ueda et al., 2004), together with Largen-O/E constructs or siRNA. Luciferase activities were measured at 48 hrs post-transfection using the Dual Luciferase Reporter Assay System (Promega). Levels of mRNAs of the luciferase reporter genes relative to 18S RNA were determined by qRT-PCR and used for normalization of luciferase activities.

### **Mitochondrial Analyses**

All mitochondrial analyses, including purification of these organelles and measurements of their mass, oxygen consumption rate, and ATP production, are described in Supplemental Experimental Procedures and Table S4.

### **Mice**

To generate Largen transgenic mice, a mouse Largen cDNA was inserted into the pCCALL2-IRES-EGFP vector (Nobak et al., 2000). The linearized plasmid was injected into fertilized (C57Bl/6 X SJL) F2 hybrid mouse eggs and two founder animals were obtained. Tissue-specific Cre-transgenic lines were obtained from The Jackson Laboratory. Mating procedures, animal care and experiments involving age-matched littermates were performed in accordance with approved institutional animal use protocols of the University Health Network.

## **Statistical Analyses**

Where appropriate, data are presented as the mean  $\pm$  SD. Significant differences between groups were determined via unpaired two-way or one-way Student t-test.

## **ACCESSION NUMBERS**

The GEO accession number for the polysomal microarray data reported in this paper is GSE54383.

## **SUPPLEMENTAL INFORMATION**

Supplemental Information includes 5 figures, 4 tables, Supplemental Experimental Procedures and Supplemental References, and can be found with this article online at...



## **ACKNOWLEDGEMENTS**

This report is dedicated to the memory of Dr. Susan McCracken, who passed away during the preparation of this manuscript. We thank Drs. Rikiro Fukunaga and Andras Nagy for plasmids; Dr. Tomoo Ogi and Mayuko Shimada for assistance with plasmid construction; Dr. David M. Sabatini and colleagues for experimental materials and fruitful discussions; and Drs. Masami Horikoshi, Akatsuki Kimura, Gerry Melino, Vuk Stambolic and Bradly Wouters for helpful input and encouragement. Finally, we are grateful to Dr. Mary Saunders for scientific editing and Denis Bouchard for cell sorting. This work was supported by a grant to Tak W. Mak from the Canadian Institutes of Health Research (#178866). This research was also funded in part by the Ontario Ministry of Health and Long Term Care. The views expressed do not necessarily reflect those of the OMOHLTC.

## REFERENCES

- Altman, P.L., and Katz, D.D. (1976) Cell biology. Federation of American Societies for Experimental Biology, Bethesda, MD.
- Bales, C.W., Davis, T.A., and Beauchene, R.E. (1988) Long-term protein and calorie restriction: alterations in nucleic acid levels of organs of male rats. *Exp. Gerontol.* 23, 189-196.
- Barberi, T., Willis, L.M., Socci, N.D., and Studer, L. (2005) Derivation of multipotent mesenchymal precursors from human embryonic stem cells. *PLoS Med.* 2, e161.
- Beretta, L., Gingras, A.C., Svitkin, Y.V., Hall, M.N., and Sonenberg, N. (1996) Rapamycin blocks the phosphorylation of 4E-BP1 and inhibits cap-dependent initiation of translation. *EMBO J.* 15, 658-664.
- Bjorklund, M., Taipale, M., Varjosalo, M., Saharinen, J., Lahdenpera, J., and Taipale, J. (2006) Identification of pathways regulating cell size and cell-cycle progression by RNAi. *Nature* 439, 1009-1013.
- Cancro, M.P. (2004) Peripheral B-cell maturation: the intersection of selection and homeostasis. *Immunol. Rev.* 197, 89-101.
- Conlon, I., and Raff, M. (1999) Size control in animal development. *Cell* 96, 235-244.
- Cook, M., and Tyers, M. (2007) Size control goes global. *Curr. Opin. Biotech.* 18, 341-350.
- Crissman, H.A., and Steinkamp, J.A. (1973) Rapid, simultaneous measurement of DNA, protein, and cell volume in single cells from large mammalian cell populations. *J. Cell Biol.* 59, 766-771.

Dowling, R.J., Topisirovic, I., Alain, T., Bidinosti, M., Fonseca, B.D., Petroulakis, E., Wang, X., Larsson, O., Selvaraj, A., Liu, Y., Kozma, S.C., Thomas, G., and Sonenberg, N. (2010) mTORC1-mediated cell proliferation, but not cell growth, controlled by the 4E-BPs. *Science* 328, 1172-1176.

Esteves, S.L., Domingues, S.C., da Cruz e Silva, O.A., Fardilha, M., and da Cruz e Silva, E.F. (2012) Protein phosphatase 1 $\alpha$  interacting proteins in the human brain. *OMICS* 16, 3-17.

Fantes, P., and Nurse, P. (1977) Control of cell size at division in fission yeast by a growth-modulated size control over nuclear division. *Exp. Cell Res.* 107, 377-386.

Fingar, D.C., Salama, S., Tsou, C., Harlow, E., and Blenis, J. (2002) Mammalian cell size is controlled by mTOR and its downstream targets S6K1 and 4EBP1/eIF4E. *Gens Dev.* 16, 1472-1487.

Fonseca, B.D., Smith, E.M., Lee, V.H., MacKintosh, C., and Proud, C.G. (2007) PRAS40 is a target for mammalian target of rapamycin complex 1 and is required for signaling downstream of this complex. *J. Biol. Chem.* 282, 24514-24524.

Greenbaum, D., Luscombe, N.M., Jansen, R., Qian, J., and Gerstein, M. (2001) Interrelating different types of genomic data, from proteome to secretome: 'oming in on function. *Genome Res.* 11, 463-468.

Guertin, D.A., Guntur, K.V., Bell, G.W., Thoreen, C.C., and Sabatini, D.M. (2006) Functional genomics identifies TOR-regulated genes that control growth and division. *Curr. Biol.* 16, 958-970.

Hervey, K.F., Zhang, X., and Thomas, D.M. (2013) The Hippo pathway and human cancer. *Nat. Rev. Cancer* 13, 246-257.

Johnston, G.C., Pringle, J.R., and Hartwell, L.H. (1977) Coordination of growth with cell division in the yeast *Saccharomyces cerevisiae*. *Exp. Cell Res.* 105, 79-98.

Jorgensen, P., Nishikawa, J.L., Breitkreutz, B.J., and Tyers, M. (2002) Systematic identification of pathways that couple cell growth and division in yeast. *Science* 297, 395-400.

Kim, S., Wong, P., and Coulombe, P.A. (2006). A keratin cytoskeletal protein regulates protein synthesis and epithelial cell growth. *Nature* 441, 362–365.

Lang, I., Schweizer, A., Hiden, U., Ghaffari-Tabrizi, N., Hagendorfer, G., Bilban, M., Pabst, M.A., Korgun, E.T., Dohr, G., and Desoye, G. (2008) Human fetal placental endothelial cells have a mature arterial and a juvenile venous phenotype with adipogenic and osteogenic differentiation potential. *Differentiation* 76, 1031-1043.

Laplante, M., and Sabatini, D.M. (2012) mTOR signaling in growth control and disease. *Cell* 149, 273-293.

Liu, D., and Songyang, Z. (2008) ERM-mediated genetic screens in mammalian cells. *Methods Enzymol.* 446, 409-419.

Loewith, R., and Hall, M.N. (2011) Target of rapamycin (TOR) in nutrient signaling and growth control. *Genetics* 189, 1177-201.

Ma, X.M., and Blenis, J. (2009) Molecular mechanisms of mTOR-mediated translational control. *Nat. Rev. Mol. Cell Biol.* 10, 307-318.

Magnuson, B., Ekim, B., and Fingar, D.C. (2012) Regulation and function of ribosomal protein S6 kinase (S6K) within mTOR signaling networks. *Biochem. J.* 441, 1-21.

Malstrom, S., Tili, E., Kappes, D., Ceci, J.D., and Tschlis, P.N. (2001) Tumor induction by an Lck-MyrAkt transgene is delayed by mechanisms controlling the size of the thymus. *Proc. Natl. Acad. Sci. USA* 98, 14967-14972.

Martin, F., Barends, S., Jaeger, S., Schaeffer, L., Prongidi-Fix, L., and Eriani, G. (2011) Cap-assisted internal initiation of translation of histone H4. *Mol. Cell* 41, 197-209.

Morita, M., Gravel, S.P., Chénard, V., Sikström, K., Zheng, L., Alain, T., Gandin, V., Avizonis, D., Arguello, M., Zakaria, C., McLaughlan, S., Nouet, Y., Pause, A., Pollak, M., Gottlieb, E., Larsson, O., St-Pierre, J., Topisirovic, I., and Sonenberg, N. (2013) mTORC1 controls mitochondrial activity and biogenesis through 4E-BP-dependent translational regulation. *Cell Metab.* 18, 698-711.

Nobak, A., Guo, C., Yang, W., Nagy, A., Lobe, C.G. (2000) Z/EG, a double reporter mouse line that expresses enhanced green fluorescent protein upon Cre-mediated excision. *Genesis* 28, 147-155.

Nurse, P. (2000) A long twentieth century of the cell cycle and beyond. *Cell* 100, 1-8.

Oh, W.J., and Jacinto, E. (2011) mTOR complex 2 signaling and functions. *Cell Cycle* 10, 2305–2316.

Persaud, A., Alberts, P., Amsen, E.M., Xiong, X., Wasmuth, J., Saadon, Z., Fladd, C., Parkinson, J., and Rotin, D. (2009) Comparison of substrate specificity of the ubiquitin ligases Nedd4 and Nedd4-2 using proteome arrays. *Mol. Syst. Biol.* 5, 333.

Postic, C., and Magnuson, M.A. (2000) DNA excision in liver by an albumin-Cre transgene occurs progressively with age. *Genesis* 26, 149–150.

Rolfe, D.F., and Brown, G.C. (1997) Cellular energy utilization and molecular origin of standard metabolic rate in mammals. *Physiol. Rev.* 77, 731-758.

Roux, P.P., and Topisirovic, I. (2012) Regulation of mRNA translation by signaling pathways. *Cold Spring Harb. Perspect. Biol.* 4, pii: a012252. doi: 10.1101/cshperspect.a012252.

Sancak, Y., Thoreen, C.C., Peterson, T.R., Lindquist, R.A., Kang, S.A., Spooner, E., Carr, S.A., and Sabatini, D.M. (2007) PRAS40 is an insulin-regulated inhibitor of the mTORC1 protein kinase. *Mol. Cell.* 25, 903-915.

Schmidt, E.E., and Schibler, U. (1995). Cell size regulation, a mechanism that controls cellular RNA accumulation: consequences on regulation of the ubiquitous transcription factors Oct1 and NF-Y and the liver-enriched transcription factor DBP. *J. Cell Biol.* 128, 467–483.

Sengupta, S., Peterson, T.R., Laplante, M., Oh, S., and Sabatini, D.M. (2010) mTORC1 controls fasting-induced ketogenesis and its modulation by ageing. *Nature* 468, 1100-1104.

Shioi, T., Kang, P.M., Douglas, P.S., Hampe, J., Yballe, C.M., Lawitts, J., Cantley, L.C., and Izumo, S. (2000) The conserved phosphoinositide 3-kinase pathway determines heart size in mice. *EMBO J.* 19, 2537-2548.

Shioi, T., McMullen, J.R., Kang, P.M., Douglas, P.S., Obata, T., Franke, T.F., Cantley, L.C., and Izumo, S. (2002) Akt/protein kinase B promotes organ growth in transgenic mice. *Mol. Cell. Biol.* 22, 2799-2809.

Sims, D., Duchek, P., and Baum, B. (2009) PDGF/VEGF signaling controls cell size in *Drosophila*. *Genome Biol.* 10, R20.

Strohecker, A.M., Guo, J.Y., Karsli-Uzunbas, G., Price, S.M., Chen, G.J., Mathew, R., and White, E. (2013) Autophagy sustains mitochondrial glutamine metabolism and growth of *Braf*<sup>V600E</sup>-driven lung tumors. *Cancer Discov.* 3, 1272-1285.

Swift, S., Lorens, J., Achacoso, P., and Nolan, G.P. (1999) Rapid production of retroviruses for efficient gene delivery to mammalian cells using 293T cell-based systems. In *Current Protocols in Immunology*, J.E. Coligan, B.E. Bierer, D.H. Margulies, E.M. Shevach, and W. Strober, eds. (New York: John Wiley & Sons), pp. 10.17.14-10.17.29.

Szabo, C., Coletta, C., Chao, C., Módis, K., Szczesny, B., Papapetropoulos, A., and Hellmich, M.R. (2013) Tumor-derived hydrogen sulfide, produced by cystathionine- $\beta$ -synthase, stimulates bioenergetics, cell proliferation, and angiogenesis in colon cancer. *Proc. Natl. Acad. Sci. USA* *110*, 12474-12479.

Thoreen, C.C., Chantranupong, L., Keys, H.R., Wang, T., Gray, N.S., and Sabatini, D.M. (2012) A unifying model for mTORC1-mediated regulation of mRNA translation. *Nature* *485*, 109-113.

Tumaneng, K., Russell, R.C., and Guan, K.L. (2012) Organ Size Control by Hippo and TOR Pathways. *Curr Biol.* *22*, R368-R379.

Tuttle, R.L., Gill, N.S., Pugh, W., Lee, J.P., Koeberlein, B., Furth, E.E., Polonsky, K.S., Naji, A., and Birnbaum, M.J. (2001) Regulation of pancreatic beta-cell growth and survival by the serine/threonine protein kinase Akt1/PKB $\alpha$ . *Nat. Med.* *7*, 1133-1137.

Ueda, T., Watanabe-Fukunaga, R., Fukuyama, H., Nagata, S., and Fukunaga, R. (2004) Mnk2 and Mnk1 are essential for constitutive and inducible phosphorylation of eukaryotic initiation factor 4E but not for cell growth or development. *Mol. Cell. Biol.* *24*, 6539-6549.

Urbani, L., Sherwood, S.W., and Schimke, R.T. (1995) Dissociation of nuclear and cytoplasmic cell cycle progression by drugs employed in cell synchronization. *Exp. Cell Res.* *219*, 159-168

Vander Haar, E., Lee, S.I., Bandhakavi, S., Griffin, T.J., and Kim, D.H. (2007) Insulin signalling to mTOR mediated by the Akt/PKB substrate PRAS40. *Nat. Cell Biol.* 9, 316-323.

Wang, J., Wilhelmsson, H., Graff, C., Li, H., Oldfors, A., Rustin, P., Brüning, J.C., Kahn, C.R., Clayton, D.A., Barsh, G.S., Thorén, P., and Larsson, N.-G. (1999) Dilated cardiomyopathy and atrioventricular conduction blocks induced by heart-specific inactivation of mitochondrial DNA gene expression. *Nature Genet.* 21, 133-137.

Warner, J.R., Knopf, P.M., and Rich, A. (1963). A multiple ribosomal structure in protein synthesis. *Proc. Natl. Acad. Sci. USA* 49, 122–129.

Yamashita, Y.M., Mahowald, A.P., Perlin, J.R., and Fuller, M.T. (2007) Asymmetric inheritance of mother versus daughter centrosome in stem cell division. *Science* 315, 518-521.

Yang, X., and Xu, T. (2011) Molecular mechanism of size control in development and human diseases. *Cell Res.* 21, 715-729.

Zhang, J., Schneider, C., Ottmers, L., Rodriguez, R., Day, A., Markwardt, J., and Schneider, B.L. (2002) Genomic scale mutant hunt identifies cell size homeostasis genes in *S. cerevisiae*. *Curr. Biol.* 12, 1992-2001.

Zid, B.M., Rogers, A.N., Katewa, S.D., Vargas, M.A., Kolipinski, M.C., Lu, T.A., Benzer, S., and Kapahi, P. (2009) 4E-BP Extends Lifespan upon Dietary Restriction by Enhancing Mitochondrial Activity in *Drosophila*. *Cell* 139, 1322-1326.



## Figure Legends

### Figure 1. A Novel Genetic Screen for Genes Controlling Mammalian Cell Size.

(A) Flow chart of the genetic screen. Please see Experimental Procedures for details. (B) Cell size distribution of control unsorted cells and 3 single clones (1C2, 3B3 and 2D10) obtained by limiting dilution. Results are representative of >3 trials. Inset numbers are the mean forward scatter (FSC) value for each group. (C) RT-PCR of the indicated mRNAs in the indicated clones and parental Jurkat cells (ctrl) after culture with (+) or without (-) DOX for 2 days. GAPDH, loading control. (D) qRT-PCR analysis of *Prr16* mRNA expression in Jurkat and 2D10 cells with (+) or without (-) DOX. (E) Cell volumes of Jurkat and *Prr16*-overexpressing clones 3B3 and 2D10 cultured with/without RAP and/or DOX. Values are the mean cell volume in picolitres  $\pm$  SD as determined by 3 independent measurements. For D and E, \* $p$ <0.05, \*\* $p$ <0.001, N.S. = not significant. See also Figure S1 and Table S1.

### Figure 2. PRR16/Largen Increases Cell Size.

(A) Cell size distribution of Jurkat cells stably overexpressing GFP or GFP-PRR16/Largen with/without RAP. The mean FSC value for each group is indicated. (B) Cell size distribution of Jurkat cells transiently transfected with siRNA against PRR16/Largen or non-targeting siControl. Analysis was performed as in (A). For A and B, results are representative of >3 trials. See also Figures S2 and S3.

### Figure 3. Largen Promotes mRNA Translation.

(A) Co-immunoprecipitation assay using anti-Myc Ab-conjugated beads and lysates of 293T

cells stably transformed with empty vector (Vector), or with plasmids expressing Myc-tagged Largin (myc-LARGEN) or Myc-tagged PRAS40 (myc-PRAS40). Proteins in the input (left), or eluted from the beads using Myc peptides (right), are shown for each lysate.  $\beta$ -actin, loading control. **(B)** Relative total protein concentrations in lysates of equal numbers of parental Jurkat and 2D10 cells cultured with/without RAP and/or DOX. Results are the mean  $\pm$  SD of values normalized to untreated Jurkat controls (n=4). **(C)** [<sup>35</sup>S]-methionine incorporation into total protein per unit time measured in Jurkat and 2D10 cells cultured with/without RAP and/or DOX. Data were normalized to values for controls without RAP and DOX, and are the mean relative translation rate  $\pm$  SD (n=3) expressed in arbitrary units (AU). **(D)** [<sup>35</sup>S]-methionine incorporation into total protein per unit time measured in control cells (-), Largin-knockdown cells (k.d.), and Largin-overexpressing cells (O/E). Results for 293T and HeLa cells are presented. Data were normalized to values for control siRNA k.d. cells or control vector transfectants and are expressed as in (C) (n=3-4). **(E)** Luciferase reporter analysis of mRNA translation in control (-) and Largin-O/E (+) 293T cells. Results are the mean absolute luciferase activity  $\pm$  SD (n=3) expressed in AU. **(F)** Translation luciferase reporter assay of HeLa cells transfected with siControl or siLargin. Data were analyzed as in (E). **(G)** Translation luciferase reporter assay of control or Largin-O/E 293T cells with/without RAP. Data were analyzed as in (E). For B-G, \* $p$ <0.05, \*\* $p$ <0.001, \*\*\* $p$ <0.0001. N.S. = not significant. See also Figure S4.

#### **Figure 4. Largin Enhances the Translation of a Specific Subset of mRNAs**

**(A)** List of mRNAs encoding mitochondrial proteins that were enriched in heavy polysome

fractions of Largen-O/E cells. **(B)** qRT-PCR analysis of the indicated transcripts in the indicated polysome fractions of control and Largen-O/E cells with/without RAP. Results are the mean mRNA level (n=3) in each fraction relative to the level in the corresponding input of the control without RAP. **(C)** Immunoblot of the indicated mitochondrial proteins in lysates of control or Largen-O/E cells with/without RAP. Results are representative of >3 trials. See also Figure S5 and Table S2.

### **Figure 5. Largen Increases Mitochondrial Mass and Respiration**

**(A)** Confocal microscopy and DIC images of two independent clones of 293T cells overexpressing Largen plus EGFP (Largen1 and Largen2), and one control clone expressing EGFP alone (Vector), which were stained with Mitotracker Red and DAPI. Scale bar, 10  $\mu$ m. **(B)** Flow cytometric measurement of mitochondrial mass in Mitotracker Red-stained control (Vector) and Largen-O/E 293T cells (Largen1 and Largen2). **(C)** Flow cytometric measurement of mitochondrial mass in Mitotracker Green-stained control Jurkat and 2D10 cells with/without DOX. For A-C, results are representative of >3 trials. For B and C, inset numbers are the mean FSC values for each group. **(D)** qRT-PCR determination of the relative copy number of mitochondrial DNA (mtDNA) compared to nuclear DNA in Jurkat and 2D10 cells with/without DOX. Results are the mean  $\pm$  SD of values normalized to the untreated control (n=3). **(E)** Oxygen consumption rates (OCR) in Jurkat and 2D10 cells with/without DOX as measured by a Seahorse analyzer. Results are the mean  $\pm$  SD from 3 independent trials, each involving multiple replicates. **(F)** Measurement of intracellular ATP content in Jurkat and 2D10 cells with/without DOX. **(G)** Measurement of intracellular ATP

content in Largen-O/E 293T cells (Largen) or control 293T cells transformed with empty vector (Vector) and treated with/without RAP. For F and G, results are the mean  $\pm$  SD (n=3). For D-G, \* $p$ <0.05, \*\* $p$ <0.001.

### **Figure 6. Mitochondrial Respiration is Linked to Cell Size Regulation**

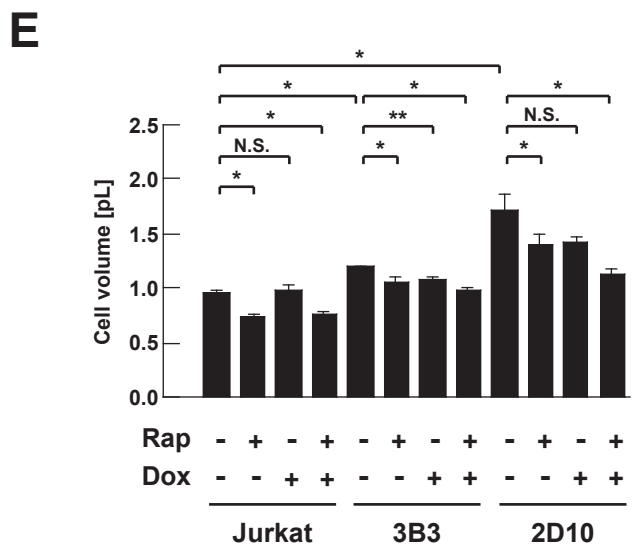
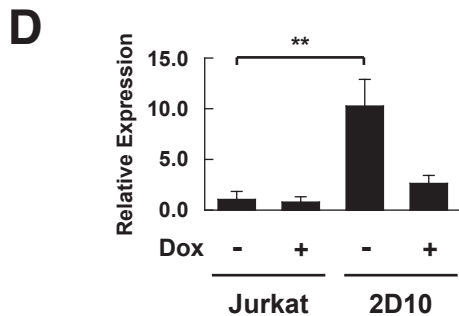
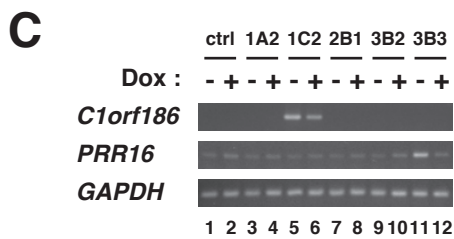
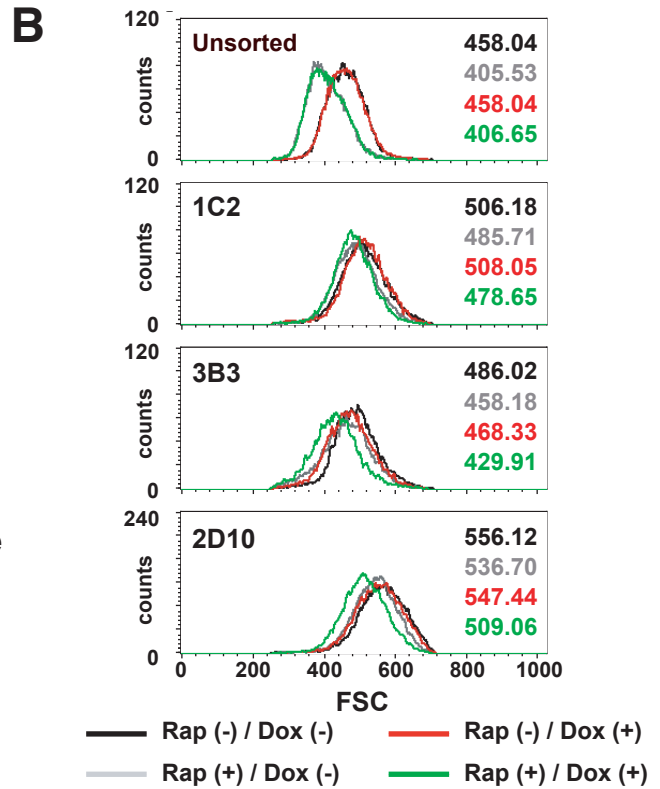
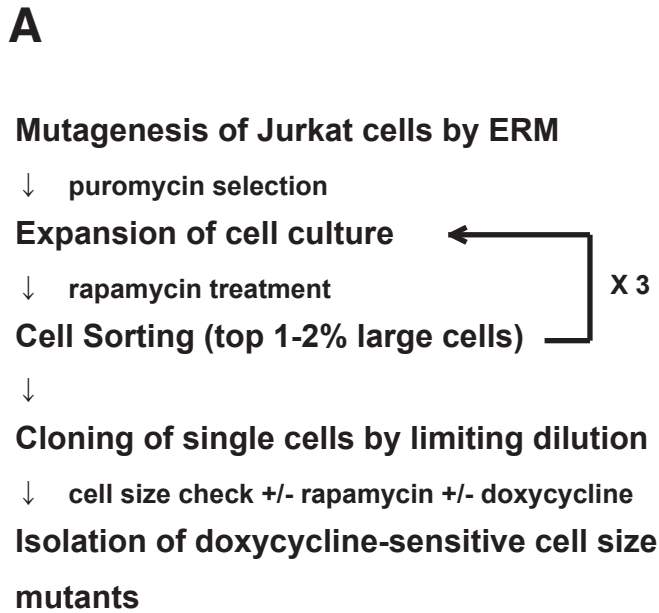
(A) Cell size distribution of Jurkat cells incubated with DMSO (vehicle) or 2  $\mu$ M carbonyl cyanide 4-(trifluoromethoxy)phenylhydrazone (FCCP). The median FSC value for each group is indicated. (B) Cell size distribution of Jurkat and 2D10 cells treated with 2  $\mu$ M FCCP with/without DOX. Analysis was performed as in (A). Results are representative of >3 trials.

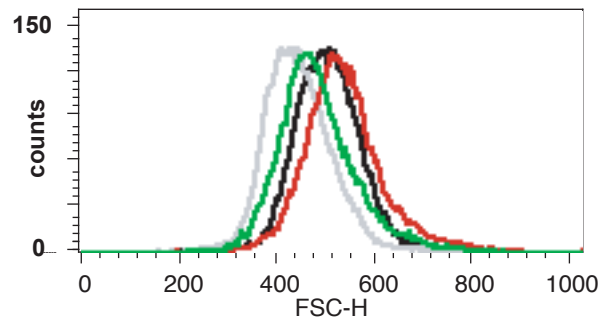
### **Figure 7. Largen Increases Cell Size *In Vivo***

(A) Two independent immunohistochemical analyses (#1, #2) of liver cross-sections from control and Largen-AlbCre littermates (n=5/group). Sections were stained with anti-cadherin Ab (brown) and haematoxylin (blue; nuclei). Scale bar, 50  $\mu$ m. (B) Cell size of hepatocytes in (A) as measured by Image-J. Results are the mean area  $\pm$  SD of 20 hepatocytes from 10 photographs of control and Largen-AlbCre mice (n=5/group) per analysis (#1, #2). (C) Copy number of mtDNA relative to nuclear DNA in hepatocytes of control and Largen-AlbCre mice determined as in Figure 5D. Results are the mean  $\pm$  SD (n=3). (D) Liver (L) and body (B) weights of the mice in (A) were measured. Results are the mean L:B ratio  $\pm$  SD expressed as a percentage (n=6). (E) Immunofluorescent microscopy of representative heart cross-sections from control and Largen-CkmmCre littermates (n=3/group). Sections were stained with Alexa Fluor 488-conjugated anti-WGA Ab. Scale bar, 50  $\mu$ m. (F) Cell size of

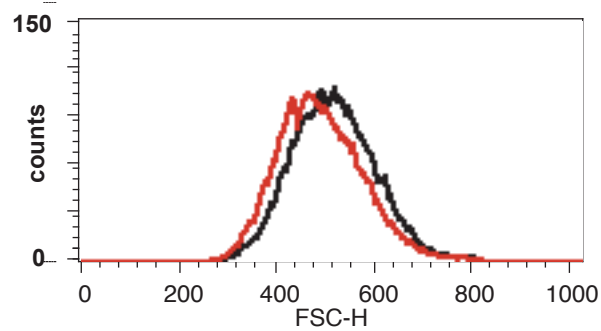
cardiomyocytes in (E) as measured by Image-J. Results are the mean area  $\pm$  SD of 10 cardiomyocytes from two photographs of control and Lagen-CkmmCre mice (n=2/group).

**(G)** Proposed model for cell size control by Lagen. Please see Discussion for details. See also Figure S6.

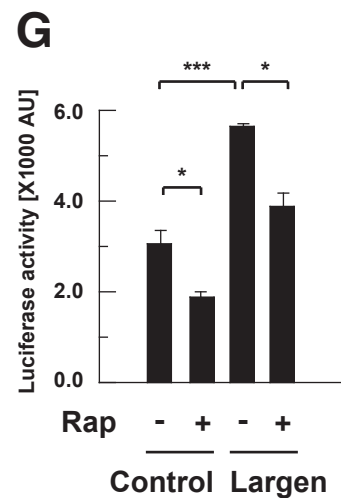
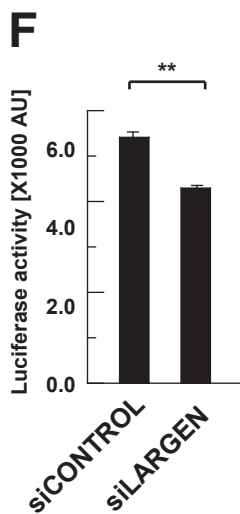
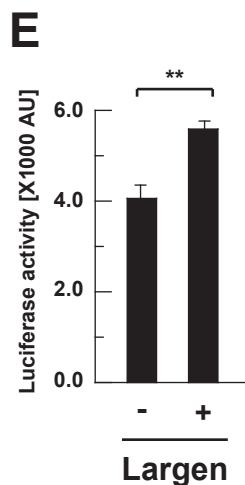
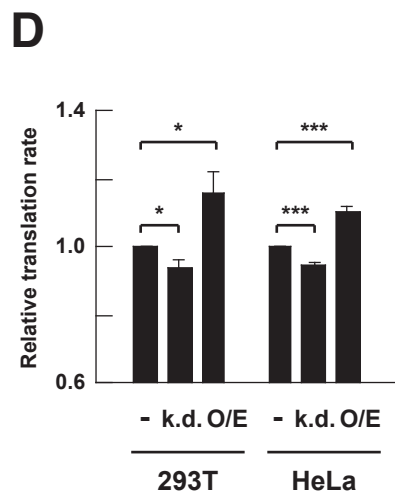
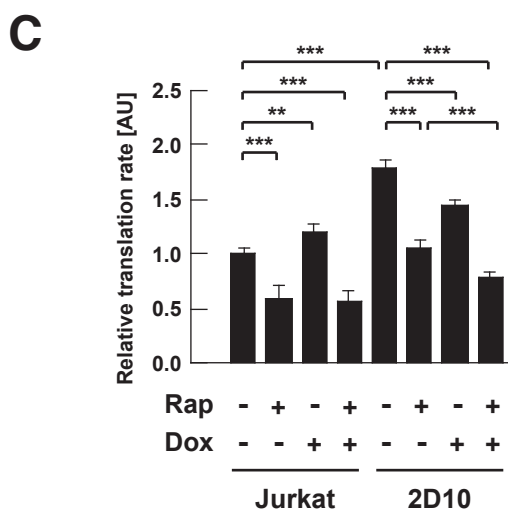
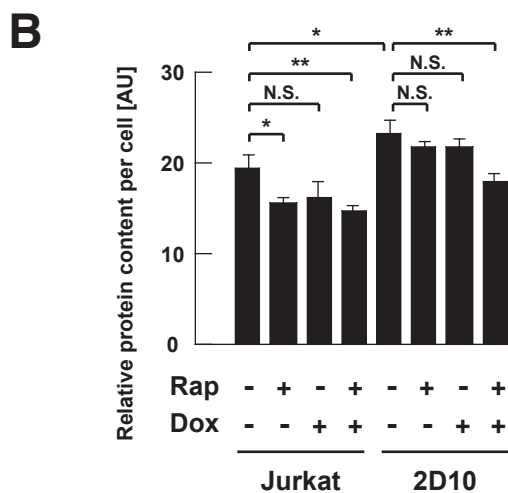
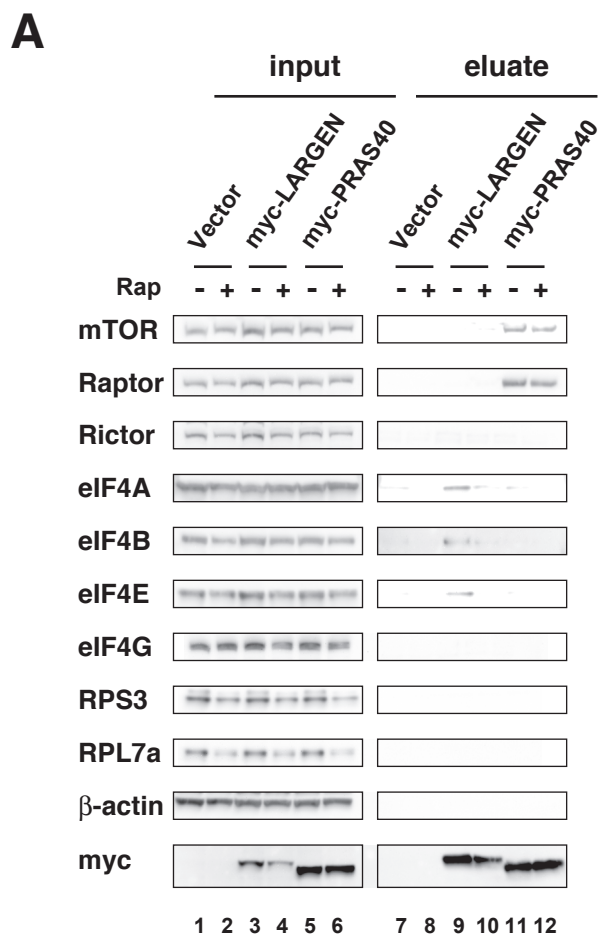


**A**

	Mean FSC
— GFP/Rap (-)	496.18
— GFP/Rap (+)	436.27
— GFP-PRR16/Rap (-)	528.44
— GFP-PRR16/Rap (+)	474.42

**B**

	Mean FSC
— siCONTROL	507.11
— siPRR16	480.45

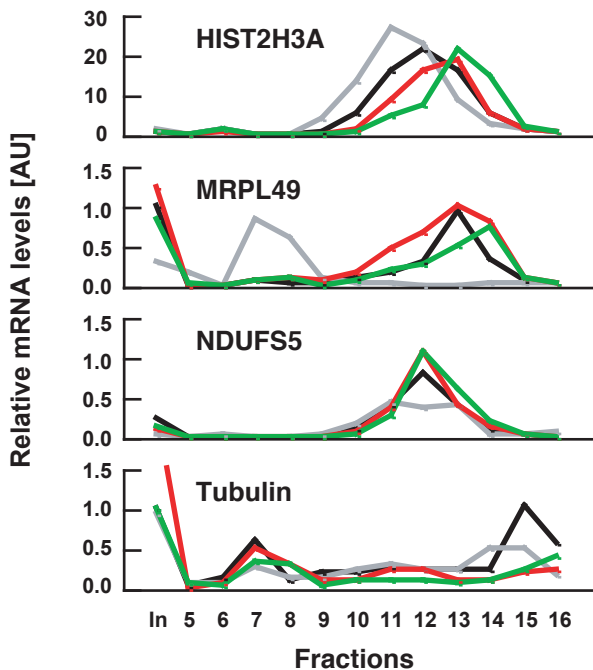




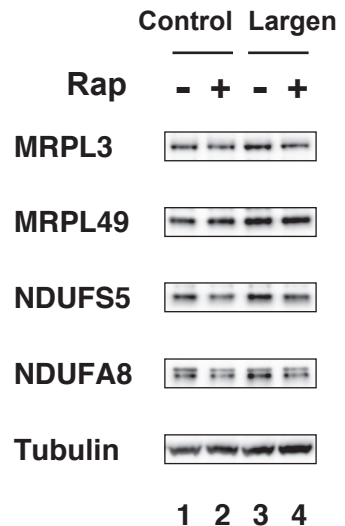
A

Gene Symbol	Description	Fold Cahnge	p-value	logFC RNA
AFG3L2	AFG3 ATPase family gene 3-like 2 (yeast) (AFG3L2), mRNA [NM_006796]	3.7662	0.00135	0.9260
C12orf65	chromosome 12 open reading frame 65 (C12orf65), mRNA [NM_152269]	3.9480	0.00031	-0.0375
CHCHD3	coiled-coil-helix-coiled-coil-helix domain containing 3 (CHCHD3), mRNA [NM_017812]	3.5508	0.01248	-0.0442
COQ4	coenzyme Q4 homolog (S. cerevisiae) (COQ4), mRNA [NM_016035]	3.7593	0.00027	0.1509
CYB5B	cytochrome b5 type B (outer mitochondrial membrane) (CYB5B), mRNA [NM_030579]	4.4443	0.00227	-0.0095
DHRS4	dehydrogenase/reductase (SDR family) member 4 (DHRS4), mRNA [NM_021004]	3.7149	0.00205	0.1356
ECH1	enoyl Coenzyme A hydratase 1, peroxisomal (ECH1), mRNA [NM_001398]	4.5475	0.00141	0.1793
ENDOGL1	endonuclease G-like 1 (ENDOGL1), mRNA [NM_005107]	5.0326	0.00489	0.0182
ERAL1	Era G-protein-like 1 (E. coli) (ERAL1), mRNA [NM_005702]	3.5932	0.00074	0.0029
GRPEL1	GrpE-like 1, mitochondrial (E. coli) (GRPEL1), mRNA [NM_025196]	4.5121	0.00029	0.3067
MLYCD	malonyl-CoA decarboxylase (MLYCD), mRNA [NM_012213]	7.3015	0.00278	-0.2882
MRPL3	mitochondrial ribosomal protein L3 (MRPL3), mRNA [NM_007208]	5.5762	0.00304	0.2104
MRPL38	mitochondrial ribosomal protein L38 (MRPL38), mRNA [NM_032478]	3.7750	0.00300	-0.0246
MRPL49	mitochondrial ribosomal protein L49 (MRPL49), mRNA [NM_004927]	5.9331	0.00037	0.2419
MRPS11	mitochondrial ribosomal protein S11 (MRPS11), mRNA [NM_022839]	3.7821	0.00797	-0.0527
NDUFS5	NADH dehydrogenase (ubiquinone) Fe-S protein 5, 15kDa, mRNA [NM_004552]	5.1960	0.00018	-0.0947
PDK3	pyruvate dehydrogenase kinase, isozyme 3 (PDK3), mRNA [NM_005391]	4.0452	0.00087	0.2448
PECR	peroxisomal trans-2-enoyl-CoA reductase (PECR), mRNA [NM_018441]	3.5096	0.00012	-0.1273
SDHC	succinate dehydrogenase complex, subunit C, 15kDa (SDHC), mRNA [NM_003001]	3.9941	0.00152	-0.2379
SH3BP5	SH3-domain binding protein 5 (BTK-associated) (SH3BP5), mRNA [NM_004844]	4.2188	0.00300	0.4223
SSBP1	single-stranded DNA binding protein 1 (SSBP1), mRNA [NM_003143]	3.5105	0.00031	-0.3311
TFAM	transcription factor A, mitochondrial (TFAM), mRNA [NM_003201]	3.6471	0.00002	-0.1576
TOMM34	translocase of outer mitochondrial membrane 34 (TOMM34), mRNA [NM_006809]	6.9715	0.00037	-0.3324
TOMM40	translocase of outer mitochondrial membrane 40 homolog, mRNA [NM_006114]	4.6797	0.00470	0.0697
TTC19	tetratricopeptide repeat domain 19 (TTC19), mRNA [NM_017775]	4.3552	0.00283	-0.0510

B

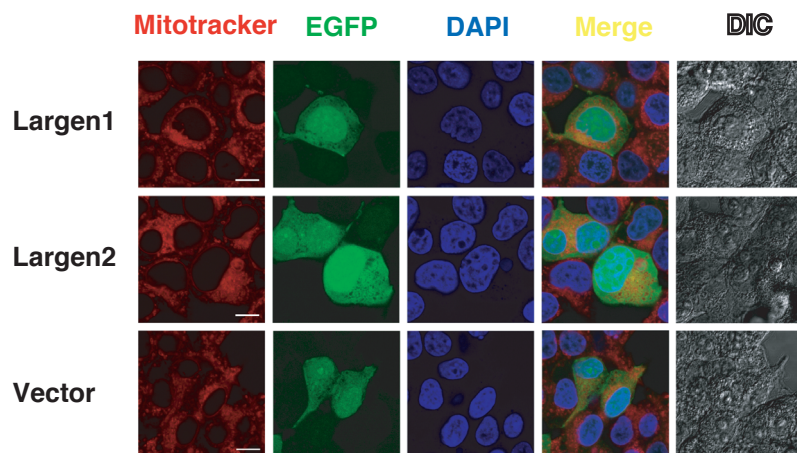


C

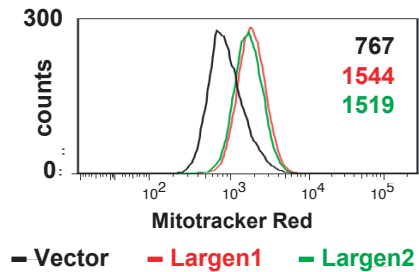


— Control / Rap (-)      — Largen / Rap (-)  
 — Control / Rap (+)      — Largen / Rap (+)

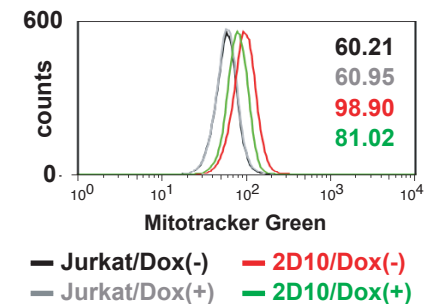
**A**



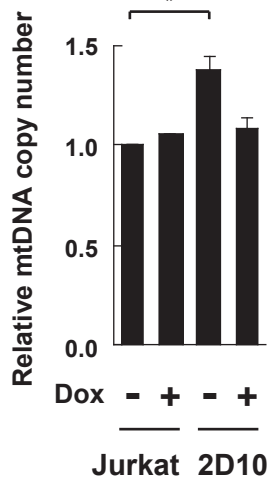
**B**



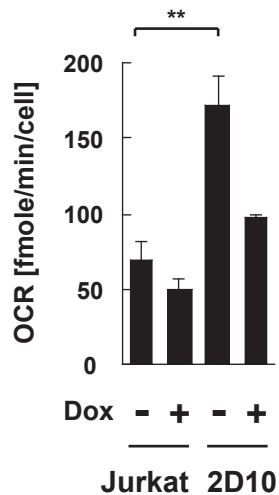
**C**



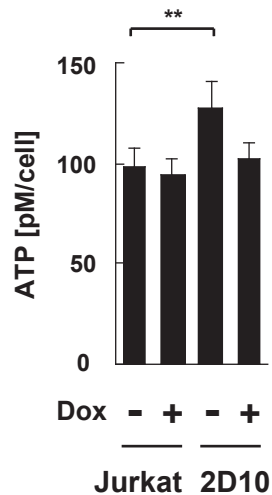
**D**



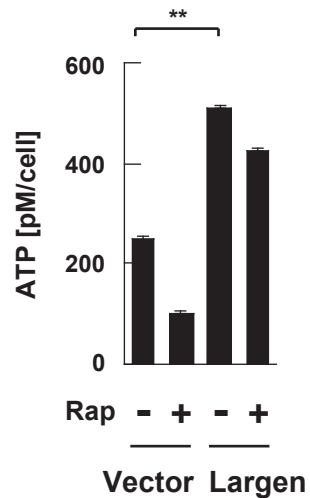
**E**



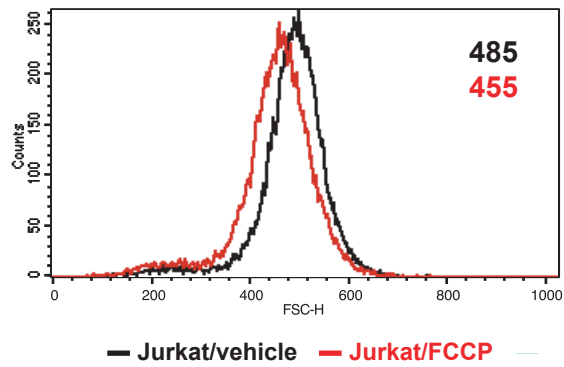
**F**



**G**



**A**



**B**

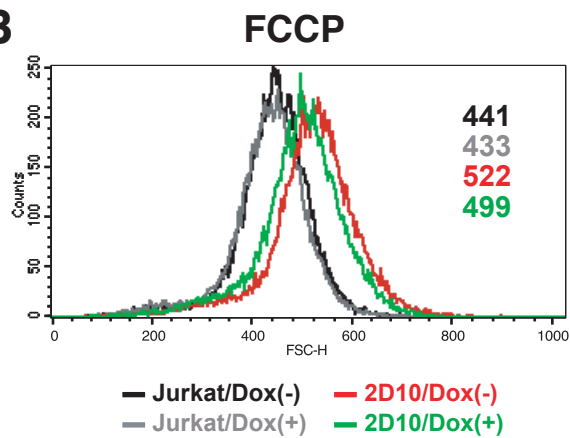
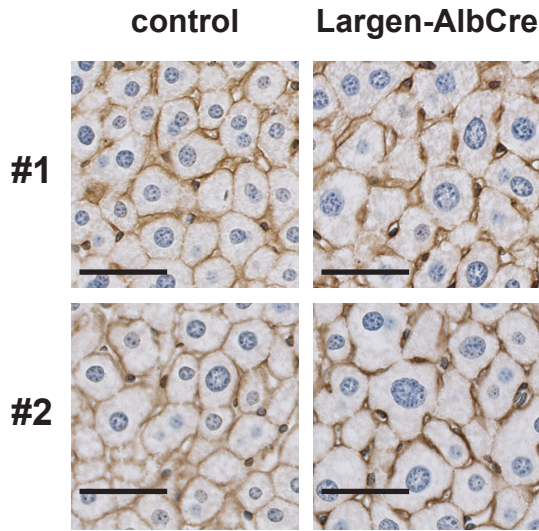
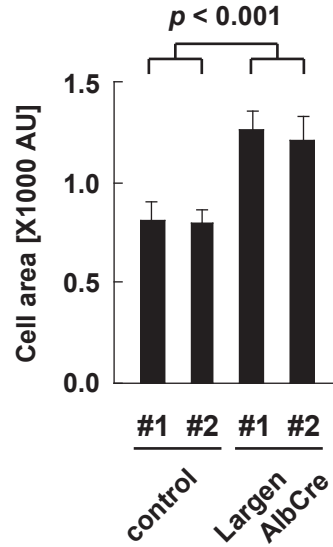


Figure 7

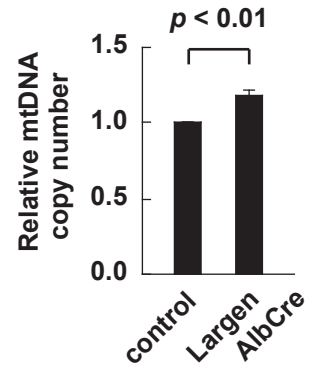
A



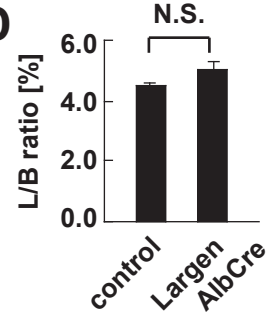
B



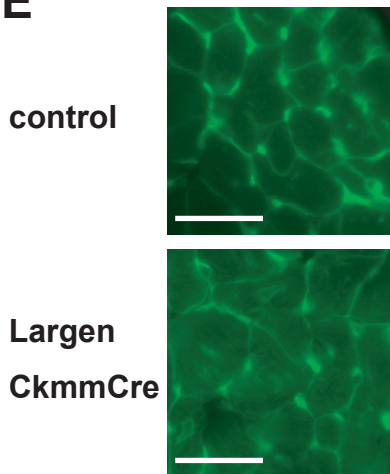
C



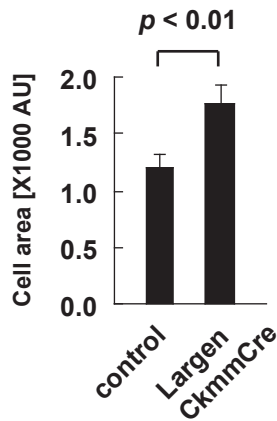
D



E



F



G

